Title: Field-based species identification in eukaryotes using real-time nanopore sequencing.

Authors: Joe Parker[1], Andrew J. Helmstetter[1], Dion Devey[1] & Alexander S.T. Papadopulos[1]

[1]Jodrell Laboratory, Royal Botanic Gardens, Kew, Richmond, Surrey UK. TW9 3AB

Correspondence to: a.papadopulos@kew.org and joe.parker@kew.org

Keywords: Nanopore, MinION, onsite DNA sequencing, phylogenomics

Advances in DNA sequencing and informatics have revolutionised biology over the past four decades, but technological limitations have left many applications unexplored[1,2]. Recently, portable, real-time, nanopore sequencing (RTnS) has become available. This offers opportunities to rapidly collect and analyse genomic data anywhere[3–5]. However, the generation of datasets from large, complex genomes has been constrained to laboratories[6,7]. The portability and long DNA sequences of RTnS offer great potential for field-based species identification, but the feasibility and accuracy of these technologies for this purpose have not been assessed. Here, we show that a field-based RTnS analysis of closely-related plant species (*Arabidopsis spp.*)[8] has many advantages over laboratory-based high-throughput sequencing (HTS) methods for species level identification-by-sequencing and *de novo* phylogenomics. Samples were collected and sequenced in a single day by RTnS using a portable, "*al fresco*" laboratory. Our analyses

demonstrate that correctly identifying unknown reads from matches to a reference database with RTnS reads enables rapid and confident species identification. Individually annotated RTnS reads can be used to infer the evolutionary relationships of *A. thaliana*. Furthermore, hybrid genome assembly with RTnS and HTS reads substantially improved upon a genome assembled from HTS reads alone. Field-based RTnS makes real-time, rapid specimen identification and genome wide analyses possible. These technological advances are set to revolutionise research in the biological sciences[9] and have broad implications for conservation, taxonomy, border agencies and citizen science.

DNA sequencing used to be a slow undertaking, but the past decade has seen an explosion in HTS methods[2,10]. DNA barcoding (i.e., the use of a few, short DNA sequences to identify organisms) has benefited from this sequencing revolution[11,12], but has never become fully portable. Samples must be returned to a laboratory for testing and the discrimination of closely related species using few genes can be problematic due to evolutionary phenomena (e.g. lineage sorting, shared polymorphism and hybridisation)[10]. While typical barcoding approaches have been effective for generic level identification, accuracy is much more limited at the species level[11,13] and concerns remain[14]. Species delimitation using limited sequencing information has also been problematic and is thought to heavily underestimate species diversity[11,15]. Consequently, increasingly elaborate analytical methods have been spawned to mitigate the inherent limitations of short sequences[13,16]. The Oxford Nanopore Technologies® MinION® is one of a new generation of RTnS DNA sequencers that is small enough to be portable for fieldwork and produces data within minutes[17,18]. These properties suggest species identification could be conducted using genome scale data generated at the point of sample collection. Furthermore, the large number of long reads generated[17] may provide more accurate species-level identification than current approaches. This application offers great potential

53 for conservation, environmental biology, evolutionary biology and combating wildlife crime,
54 however, this potentially exciting combination of methods has not yet been tested in the
55 field for eukaryotes.

56 Our experiment was designed to determine whether DNA reads produced entirely in
57 the field could accurately identify and distinguish samples from closely-related species (*A.*
58 *thaliana* (L.) Heynh. and *A. lyrata* (L.) O'Kane & Al-Shehbaz). Recent analyses have
59 shown that gene flow has been common and shared polymorphisms are abundant
60 between the morphologically distinct species in *Arabidopsis.* Indeed, the two study species
61 share >20,000 synonymous SNPs[8], making this a good stress test of genome scale RTnS
62 sequencing for species discrimination.

63 The first goal was to extract and sequence shotgun genomic data from higher plant
64 species in the field using RTnS technology in sufficient quantity for downstream analyses
65 within hours of the collection of plant tissue (Extended Figure 1). On consecutive days,
66 tissue was collected from three specimens each of *A. thaliana* and *A. lyrata subsp. petraea*
67 (Figs. 1b,c) in Snowdonia National Park, and prepared, sequenced and analysed
68 outdoors in the Croesor Valley (Fig. 1a). Only basic laboratory equipment was used for
69 DNA extraction and MinION sequencing-library preparation; we did not use a PCR
70 machine (Fig. 1d; Extended Data Table 1). One specimen of each species was sequenced
71 with both R7.3 and R9 MinION chemistries. For *A. thaliana,* the RTnS experiment
72 generated 97k reads with a total yield of 204.6Mbp over fewer than 16h of sequencing
73 (see Extended Data Table 2). Data generation was slower for *A. lyrata*, over ~90h
74 sequencing (including three days of sequencing at RBG Kew following a 16h drive), 26k
75 reads were generated with a total yield of 62.2Mbp. At the time, a limited implementation
76 of local basecalling was available for the R7.3 data only. Of 1,813 locally basecalled reads,
77 281 had successful BLAST matches to the reference databases with a correct to incorrect
78 species ID ratio of 223:30. The same samples were subsequently sequenced using HTS

79 short read technology (Illumina MiSeq™, paired-end, 300bp; Supplementary note 1).
80 Mapping reads to available reference genomes for the *A. thaliana* (TAIR10 release[19]) and
81 two *A. lyrata* assemblies[20,21] indicates approximate RTnS coverage of 2.0x, 0.3x, and 0.3x
82 for *A. thaliana*, *A. lyrata*, and *A. lyrata ssp. petraea*, respectively; and 19.5x, 11.9x and
83 12.0x respectively for HTS reads (Extended Data Tables 2 and 3, Supplementary note 2).
84 These results demonstrate that the entire process (from sample collection thorough to
85 genome scale sequencing) is now feasible for eukaryotic species within a few hours in
86 field conditions. As the technology develops, run yields are expected to improve and
87 implementation of sample indexing will allow many samples to be run on a single flow cell.

88 As expected given the developmental stages of the technologies, the quality and
89 yield of field sequenced RTnS data was lower than the HTS data (Extended Data Tables 2
90 and 4). *Arabidopsis thaliana* RTnS reads could be aligned to approx. 50% of the reference
91 genome (53Mbp) with an average error rate of 20.9%. Indels and mismatches were
92 present in similar proportions. The *A. lyrata* RTnS data were more problematic with
93 significantly poorer mapping to the two *A. lyrata* assemblies, whereas, the HTS data
94 performed relatively well. For the limited number of alignable RTnS reads, error rates were
95 slightly higher than for *A. thaliana* (22.5% and 23.5%). The poorer RTnS results for *A.*
96 *lyrata* may be a consequence of temperature-related reagent degradation in the field or
97 due to unknown contaminants in the DNA extraction that inhibited library preparation
98 and/or RTnS sequencing. Despite the smaller yield and lower accuracy of the RTnS
99 compared to HTS data, the RTnS reads were up to four orders of magnitude longer than
100 the HTS reads and we predicted they would be useful for species identification, hybrid
101 genome assembly and phylogenomics.

102 To explore the utility of these data for species identification, the statistical
103 performance of field-sequenced (RTnS) and lab-sequenced (HTS) read data was
104 assessed. Datasets for each species were compared to two databases via BLASTN,

105 retaining single best-hits: one database contained the *A. thaliana* reference genome and
106 the second was composed of the two draft *A. lyrata* genomes combined. Reads which
107 matched a single database were counted as positive matches for that species. The
108 majority of matching reads hit both databases, which is expected given the close
109 evolutionary relationships of the species. In these cases, positive identifications were
110 determined based on four metrics; a) the longest alignment length, b) the highest %
111 sequence identities and c) the largest number of sequence identities d) the lowest *E*-value
112 (Extended Data Table 4). Test statistics for each of these metrics were calculated as the
113 difference of scores (length, % identities, or *E*-value) between 'correct' and 'incorrect'
114 database matches. The performance of these difference statistics for binary classification
115 was assessed by investigating the true and false positive rates (by reference to the known
116 sample species) across a range of threshold difference values (Fig. 2a-d and Extended
117 Data Figs. 2-4). For both short- and long-read data at thresholds greater than 100bp, the
118 differences in total alignment lengths (ΔL_T) or number of identities (ΔL_I) are superior to e-
119 value or % identity biases (Figs. 2a-d). Furthermore, at larger thresholds (i.e., more
120 conservative tests), RTnS reads retained more accuracy in true- and false-positive
121 discrimination than HTS data. This proves that whole genome shotgun RTnS is a powerful
122 method for species identification. We posit that the extremely long length of the observed
123 'true positive' alignments compared with an inherent length ceiling on false-positive
124 alignments in a typical BLASTn search is largely responsible for this property.

125 To evaluate the speed with which species identification can be carried out, we
126 performed *post hoc* analyses by subsampling the RTnS *A. thaliana* dataset. This simulated
127 the rate of improvement in species assignment confidence over a short RTnS run. We
128 classified hits among the subsampled reads based on (i) ΔL_I over a range of threshold
129 values (ii) mean ΔL_I and (iii) aggregate ΔL_I (Fig. 3). This demonstrates that a high degree
130 of confidence can be assigned to species identifications over the timescales needed to

131 generate this much data (i.e., < one hour) and that variation in the accuracy of
132 identifications quickly stabilises above 1000 reads. Aggregate ΔL_l values rapidly exclude
133 zero (no signal) or negative (incorrect assignment) values, making this simple and rapidly-
134 calculated statistic particularly useful for species identification. In a multispecies context,
135 the slopes of several such log-accumulation curves could be readily compared, for
136 example (see Supplementary Discussion).

137 Assembly of large and complicated eukaryotic genomes with RTnS data alone
138 would require a greater volume of data than available here[7,22–24]. Field extracted samples
139 are unlikely to be of similar purity to those obtained with more sophisticated laboratory-
140 based methods, leading to lower yields. As expected, *de novo* assembly of our RTnS data
141 performed poorly, likely due to insufficient coverage. However, these data do have
142 potential for hybrid genome assembly approaches. We assembled the HTS data *de novo*
143 using ABYSS[25] and produced a hybrid assembly with both RTnS and HTS datasets using
144 HybridSPAdes[26]. The hybrid assembly was an improvement over the HTS-only assembly
145 (see Extended Data Table 5) with fewer contigs, a total assembly length closer to the
146 reference (119.0Mbp), N50 and longest contig statistics both increasing substantially and
147 estimated completeness (CEGMA[27]) of coding loci increased to ~99%. These results
148 suggest that relatively small quantities of long and short reads can produce useful genome
149 assemblies when analysed together, an important secondary benefit of field–sequenced
150 data. The length of typical RTnS reads is similar to that of genomic coding sequences (1-
151 10kb)[17]. This raises the possibility of extracting useful phylogenetic signal from such data,
152 despite the relatively high error rates of individual reads. We annotated individual raw *A.*
153 *thaliana* reads directly, without genome assembly, which recovered over 2,000 coding loci
154 from the data sequenced in the first three hours (Fig. 2e). These predicted gene
155 sequences were combined with a published dataset spanning 852 orthologous, single-
156 copy genes[28], downsampled to 6 representative taxa. Of our gene models, 207 were

157 present in the Wickett *et al.*[28] dataset and the best 56 matches were used for
158 phylogenomic analysis (see Supplementary Methods for details). The resulting
159 phylogenetic trees (Fig. 2f and Extended Data Fig. 5) are consistent with the established
160 intergeneric relationships[28]. Although the taxonomic scale used here for phylogenomics is
161 coarse it highlights an additional benefit to rapid, in-the-field sequencing for evolutionary
162 research.

163 This experiment is the first to demonstrate field-based sequencing of higher plant
164 species. When directly compared to lab-based HTS, our experiment highlights key
165 discriminatory metrics for highly accurate species identifications using portable RTnS
166 sequencing. Few approaches can boast this level of discriminatory power and none of
167 these have the same degree of portability[10,11]. The data produced for identification is also
168 useful for genome assembly. Entire coding sequences can be recovered from single reads
169 and incorporated into evolutionary analyses. Clearly, data generated with the goal of
170 accurate species identification has much broader usefulness for genomic and evolutionary
171 research. Few technical barriers remain to prevent the adoption of portable RTnS by non-
172 specialists, or even keen amateurs and schoolchildren. As these tools mature, and the
173 number of users expands, portable RTnS sequencing can revolutionise the way in which
174 researchers and practitioners can approach ecological, evolutionary and conservation
175 questions.

176 **Methods summary:** Genomic DNA was extracted from two plant specimens and
177 sequenced on Oxford Nanopore MinION devices according to manufacturers'
178 recommendations in a portable outdoor laboratory. Offline basecalling software and local
179 BLAST (v2.2.31) were used to identify individual reads on-site. Short reads were
180 sequenced in the laboratory from the same extracted DNA using an Illumina MiSeq. Local
181 BLAST was used to identify reads from all four datasets (2 field x 2 species) by
182 comparison to available published reference genomes. Gene models were predicted

183 directly from individual DNA reads using SNAP (v2006-07-28), matched to existing
184 phylogenomic datasets and used to infer plant phylogenies using MUSCLE (v3.8.31) and
185 RAxML (v7.2.8). *de novo* genome assemblies were performed using Abyss (v1.5.2) and
186 Hybrid-SPAdes (v3.5.1) with completeness assessed with QUAST (v4.0) and CEGMA. R
187 (v3.1.3) was used to perform statistical analyses. Additional details are given in the
188 Supplementary Methods.
189
190 **References:**

191 1. Hebert, P. D. N., Hollingsworth, P. M., Hajibabaei, M. & Hebert, P. D. N. From
192 writing to reading the encyclopedia of life. *Philos. Trans. R. Soc. London B Biol. Sci.*
193 **371,** 1–9 (2016).
194 2. Hajibabaei, M., Baird, D. J., Fahner, N. A., Beiko, R. & Golding, G. B. A new way to
195 contemplate Darwin's tangled bank: how DNA barcodes are reconnecting
196 biodiversity science and biomonitoring. *Philos. Trans. R. Soc. London B Biol. Sci.*
197 **371,** 20150330 (2016).
198 3. Quick, J. *et al.* Real-time, portable genome sequencing for Ebola surveillance.
199 *Nature* **530,** 228–32 (2016).
200 4. Faria, N. R. *et al.* Mobile real-time surveillance of Zika virus in Brazil. *Genome Med.*
201 **8,** 97 (2016).
202 5. Edwards, A., Debbonaire, A. R., Sattler, B., Mur, L. A. & Hodson, A. J. Extreme
203 metagenomics using nanopore DNA sequencing: a field report from Svalbard, 78 N.
204 *bioRxiv* 73965 (2016). doi:10.1101/073965
205 6. Schmidt, K. *et al.* Identification of bacterial pathogens and antimicrobial resistance
206 directly from clinical urines by nanopore-based metagenomic sequencing. *J.*
207 *Antimicrob. Chemother.* dkw397 (2016). doi:10.1093/jac/dkw397
208 7. Datema, E. *et al.* The megabase-sized fungal genome of Rhizoctonia solani

209 assembled from nanopore reads only. *bioRxiv* (2016). doi:10.1101/084772
210 8. Novikova, P. Y. *et al.* Sequencing of the genus Arabidopsis identifies a complex
211 history of nonbifurcating speciation and abundant trans-specific polymorphism. *Nat.*
212 *Genet.* **48,** 1077–1082 (2016).
213 9. Erlich, Y. A vision for ubiquitous sequencing. *Genome Res.* **25,** 1411–1416 (2015).
214 10. Mallo, D. & Posada, D. Multilocus inference of species trees and DNA barcoding.
215 *Philos. Trans. R. Soc. London B* **371,** 20150335 (2016).
216 11. CBOL Plant Working Group *et al.* A DNA barcode for land plants. *Proc. Natl. Acad.*
217 *Sci. U. S. A.* **106,** 12794–7 (2009).
218 12. Hollingsworth, P. M., Li, D.-Z., van der Bank, M. & Twyford, A. D. Telling plant
219 species apart with DNA: from barcodes to genomes. *Philos. Trans. R. Soc. B Biol.*
220 *Sci.* **371,** 20150338 (2016).
221 13. Little, D. P. DNA barcode sequence identification incorporating taxonomic hierarchy
222 and within taxon variability. *PLoS One* **6,** (2011).
223 14. Collins, R. A. & Cruickshank, R. H. The seven deadly sins of DNA barcoding. *Mol.*
224 *Ecol. Resour.* **13,** 969–975 (2013).
225 15. Tang, C. Q. *et al.* The widely used small subunit 18S rDNA molecule greatly
226 underestimates true diversity in biodiversity surveys of the meiofauna. *Proc. Natl.*
227 *Acad. Sci.* **109,** 16208–16212 (2012).
228 16. Zhang, A. B. *et al.* A fuzzy-set-theory-based approach to analyse species
229 membership in DNA barcoding. *Mol. Ecol.* **21,** 1848–1863 (2012).
230 17. Laver, T. *et al.* Assessing the performance of the Oxford Nanopore Technologies
231 MinION. *Biomol. Detect. Quantif.* **3,** 1–8 (2015).
232 18. Kasianowicz, J. J., Brandin, E., Branton, D. & Deamer, D. W. Characterization of
233 individual polynucleotide molecules using a membrane channel. *Proc. Natl. Acad.*
234 *Sci. U. S. A.* **93,** 13770–3 (1996).

235 19. Lamesch, P. *et al.* The Arabidopsis Information Resource (TAIR): improved gene
236 annotation and new tools. *Nucleic Acids Res.* **40,** D1202–D1210 (2012).
237 20. Hu, T. T. *et al.* The Arabidopsis lyrata genome sequence and the basis of rapid
238 genome size change. *Nat. Genet.* **43,** 476–81 (2011).
239 21. Akama, S., Shimizu-Inatsugi, R., Shimizu, K. K. & Sese, J. Genome-wide
240 quantification of homeolog expression ratio revealed nonstochastic gene regulation
241 in synthetic allopolyploid Arabidopsis. *Nucleic Acids Res.* **42,** (2014).
242 22. Goodwin, S., Gurtowski, J., Ethe-sayers, S., Deshpande, P. & Michael, C. Oxford
243 Nanopore Sequencing and de novo Assembly of a Eukaryotic Genome. (2015).
244 23. Mikheyev, A. S. & Tin, M. M. Y. A first look at the Oxford Nanopore MinION
245 sequencer. *Mol. Ecol. Resour.* **14,** 1097–1102 (2014).
246 24. Jansen, H. J. *et al.* Rapid de novo assembly of the European eel genome from
247 nanopore sequencing reads. *bioRxiv* (2017). doi:10.1101/101907
248 25. Simpson, J. T., Wong, K., Jackman, S. D., Schein, J. E. & Jones, S. J. M. ABySS : A
249 parallel assembler for short read sequence data ABySS : A parallel assembler for
250 short read sequence data. 1117–1123 (2009). doi:10.1101/gr.089532.108
251 26. Antipov, D., Korobeynikov, A., McLean, J. S. & Pevzner, P. A. HybridSPAdes: An
252 algorithm for hybrid assembly of short and long reads. *Bioinformatics* **32,** 1009–1015
253 (2016).
254 27. Parra, G., Bradnam, K. & Korf, I. CEGMA: A pipeline to accurately annotate core
255 genes in eukaryotic genomes. *Bioinformatics* **23,** 1061–1067 (2007).
256 28. Wickett, N. J. *et al.* Phylotranscriptomic analysis of the origin and early diversification
257 of land plants. *Proc. Natl. Acad. Sci.* **111,** E4859–E4868 (2014).
258
259 **Supplementary Information** is linked to the online version of the paper.

Acknowledgements This work was funded by a Pilot Study Grant to JDP and a Howard Lloyd Davies legacy grant to ASTP. JDP was also supported by funding from the Calleva Foundation Phylogenomic Research Programme and the Sackler Trust. The authors also thank The Botanical Society of Britain & Ireland. Natural Resources Wales, Tim Wilkinson, Robyn Cowan, and Patricia and David Brandwood for assistance.

Author contributions ASTP and JDP conceived the study and obtained funding. ASTP, DD and JDP designed and conducted fieldwork. ASTP designed and conducted field-based labwork with input from JDP, AH and DD. AH conducted lab-based sequencing. JDP conducted bioinformatics and phylogenomic analyses with contributions from AH. ASTP and JDP prepared the manuscript with contributions from DD and AH.

Author information Basecalled read data for Illumina and Oxford Nanopore sequencing runs are available via the EBI ENA at XXXXX. The authors declare competing financial interests: Oxford Nanopore Technologies contributed MinION sequencing reagents and flowcells for this research. JDP and ASTP received travel remuneration and free tickets to present an early version of this work at a conference (London Calling 2016). Correspondence and requests for materials should be addressed to ASTP (a.papadopulos@kew.org) and JDP (joe.parker@kew.org).

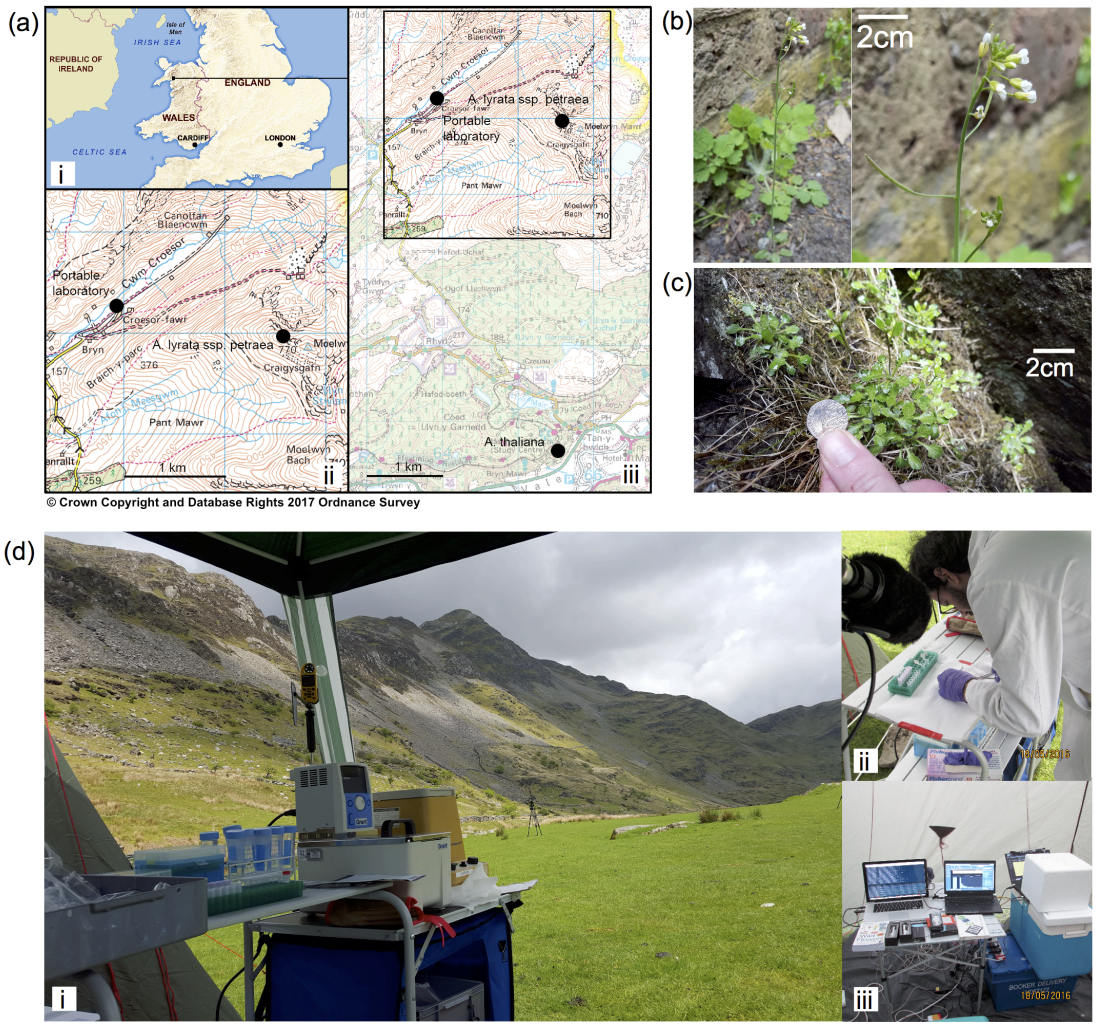

Figure 1 | Logistics and scope of field-based sequencing. a, Location of sample collection and extraction, sequencing and analyses in the Snowdonia National Park, Wales. **b,** *Arabidopsis thaliana*. **c,** *A. lyrata ssp. petraea*. **d,** The portable field laboratory used for the research. Ambient temperatures varied between 7-16ºC with peak humidity >80%. A portable generator was used to supply electrical power.

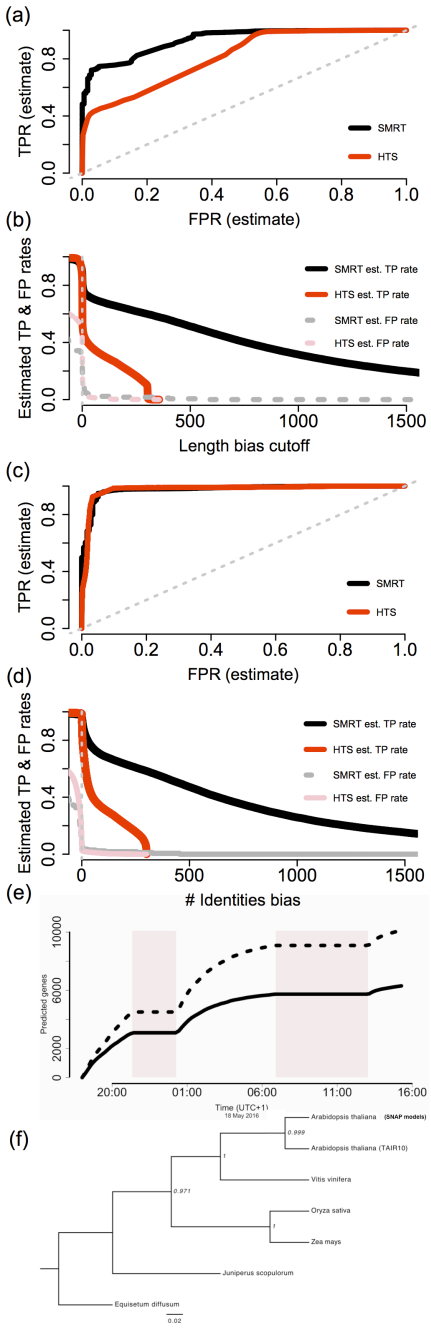

Figure 2 | Sample identification and phylogenomics using field-sequenced RTnS data. a-d Orthogonal species identification using BLASTN difference statistics: HTS data (red) and RTnS (black) matched to reference databases via BLASTN. **a, c** Receiver operating characteristic (ROC; estimated false-positive rate vs. estimated true positive rate) and **b, d** estimated true- (solid lines) and false-positive (dashed lines) rates. **a, b** ΔL_T statistic; **c, d,** ΔL_I statistic. **e,** Accumulation curves for *ab initio* gene models predicted directly from individual *A. thaliana* reads over time. Count of unique TAIR10 genes (solid

296 line) and total number of gene models (dashed line). Shaded boxes represent periods
297 where the MinION devices were halted while the laboratory was dismantled and moved. **f,**
298 phylogenetic tree inferred under the multispecies coalescent from RTnS reads.
299
300

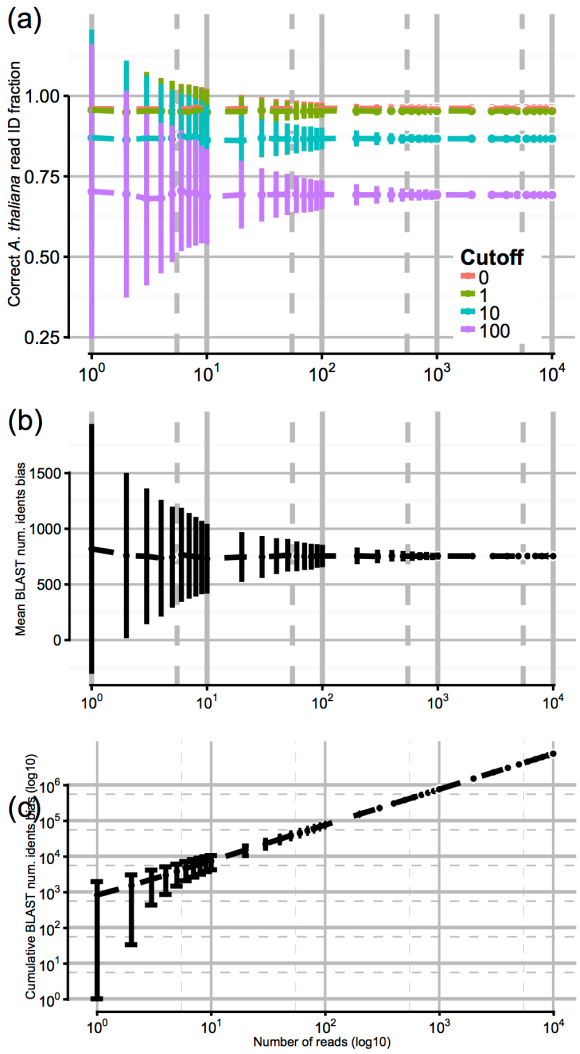

Figure 3 | Simulated accumulation curves for rapid species identification by DNA sequencing. 34k pairwise BLASTN hits of *A. thaliana* RTnS reads were subsampled without replacement to simulate an incremental accumulation of data (10^4 reads; 10^3 replicates). For each read the total identities bias (ΔL_I) is the number of identities with the *A. thaliana* reference minus the number of identities with the *A. lyrata* reference. **a)** the proportion of *A. thaliana* reads correctly identified on a per-read basis, classified as *A. thaliana* where ΔL_I > threshold cutoff (0, 1, 10 or 100). **b)** Mean ΔL_I in the simulated dataset rapidly stabilises on the population mean (+754bp, e.g. an average matching read alignment to *A. thaliana* is 754bp longer than to *A. lyrata*). **c)** Cumulative aggregate Δ_{LI}; negative or zero ΔL_I can rapidly be excluded. Typical data throughput rates exceed 10^4 reads per hour of sequencing.

312

313 **Extended Methods**

314 **Study site and sample collection.** On consecutive days, tissue was collected from three
315 specimens each of *A. thaliana* and *A. lyrata subsp. petraea* in Snowdonia National Park
316 and sequenced and analysed in a tent. *A. lyrata* was collected from the summit of
317 Moelwyn Mawr (52.985168° N, 4.003754° W; OL17 65554500; SH6558244971) and
318 *Arabidopsis thaliana* was collected at Plâs Tan-y-Bwlch (52.945976° N 4.002730° W;
319 OL18 65604060; SH6552940610). Representative voucher specimens of each species
320 are deposited at RBG, Kew. DNA extractions, library preparation and DNA sequencing
321 with the MinION technology were all conducted using portable laboratory equipment in the
322 Croesor valley on the lower slopes of Moelwyn Mawr immediately following sample
323 collection (52.987463°N 4.028517° W; OL17 63904530; SH6392745273). Laboratory
324 reagents were stored in passively-cooled polystyrene boxes with internal temperatures
325 monitored using an Arduino Uno. Only basic laboratory equipment was used (including two
326 MinION sequencers and three laptops; see Extended Data Table 1).

327 **DNA extraction.** The standard Qiagen DNeasy plant mini prep kit was used to extract
328 genomic DNA from *Arabidopsis spp.* with the exception that the two batches were pooled
329 at the DNeasy mini spin column step to maximise the DNA yield.

330 **DNA library preparation and sequencing.** An R7.3 and R9 1D MinION library
331 preparation were performed for each species according to the manufacturer's instructions
332 using a developer access programme version of the commercially available Nanopore
333 RAD-001 library kit (Oxford Nanopore Technologies). No PCR machine was used.
334 Lambda phage DNA was added to *A. thaliana* R9 library for quality control. For *A. thaliana,*
335 the MinION experiment generated 96,845 1D reads with a total yield of 204.6Mbp over
336 fewer than 16h of sequencing. Data generation was slower for *A. lyrata*, possibly due to

337 temperature-related reagent degradation or unknown contaminants in the DNA extraction.
338 Over ~90h sequencing, 25,839 1D reads were generated with a total yield of 62.2Mbp; this
339 included three days of sequencing at RBG Kew following a 16h drive, during which
340 reagents and flowcell were stored sub-optimally (near room-temperature). BLASTN 2.4.0[29]
341 was used to remove 5,130 reads with identity to phage lambda. Data are given in
342 Extended Data Table 2. The following week in a laboratory, NEBNext Ultra II sequencing
343 libraries were prepared for four field-extracted samples (two individuals from each species)
344 and sequenced on an Illumina MiSeq (300bp, paired end). In total, 11.3Gbp and 37.8M
345 reads were generated (each ~ 8M reads and 2Gbp; see Supplementary Note 1).

346 **Field offline basecalling and bioinformatics in real-time.** Offline basecalling using
347 nanocall 0.6.13[30] was applied to the R7.3 data as no offline R9 basecaller was available at
348 the time. Basecalled reads were compared to the reference genomes of *A. thaliana*
349 (TAIR10 release) and *A. lyrata subsp petraea* (1.0 release). In total, 119 reads were
350 processed in real-time with six reads making significant hits by BLASTN that scored
351 correctly : incorrectly for species ID in a 2:1 ratio. After the sequencer had been halted a
352 larger dataset of 1,813 reads gave 281 hits, with correct : incorrect : tied identifications in a
353 223:30:28 ratio.

354 **Accuracy and mapping rates of short- and long-read data.** Both lab-sequenced NGS
355 reads (trimmed with Trimmomatic[31]) and untrimmed, field-sequenced RTnS reads were
356 aligned to the appropriate reference genomes using the BWAv0.7.12-r1039[32] and
357 LASTv581[33] , to estimate depth of coverage and nominal error rate in mapped regions
358 (see Supplementary Note 2). For all *A. thaliana* datasets (short and long-read), average
359 mapped read depths were approximately equal to the gross coverage. MinION reads could
360 be aligned to 53Mbp of the reference genome with LAST (approx. 50% of the total genome
361 length). The nominal average error rate in these alignments was 20.9%). For both MinION
362 and MiSeq datasets, mapping and alignment to the *A. lyrata* and *A. lyrata ssp. petraea*

363 assemblies was more problematic. For alignable MinION reads, error rates were slightly
364 higher than for *A. thaliana* at 22.5% and 23.5%, estimated against *A. lyrata* and *A. lyrata*
365 *ssp. petraea* assemblies, respectively. We note that these assemblies are poorer quality
366 than the *A. thaliana* TAIR10 release; total genome lengths differ (206Mbp and 202Mbp,)
367 and contiguity is relatively poor in both (695 and 281,536 scaffolds).

368 **Determination of true- and false-positive detection rates, sensitivity, and specificity.**
369 Each of the four datasets (HTS and RTnS, for each species) was matched against two
370 custom databases (the *A. thaliana* reference genome and the two draft *A. lyrata* genomes
371 combined) separately with BLASTN, retaining only the best hit for each query. Queries
372 matching only a single database were counted as positive matches for that species
373 (Extended Data Table 4). Non-matching reads were treated as negative results
374 (Supplementary Methods). Queries matching both databases were defined as positives
375 based on: a) longest alignment length (L_T); b) highest % sequence identities, c) longest
376 alignment length counting only identities (L_I), or c) lowest E-value. Test statistics for each
377 of these metrics were simply calculated as the difference of scores (length (ΔL_T), %
378 identities, identities (ΔL_I), or E-value) between 'true' and 'false' hits. The statistical
379 performance of these statistics (true- and false-positive rates, and accuracy) in putative
380 analyses under varying threshold values were calculated and visualized using the ROCR
381 package in R[34]. The high proportion of reads with significant hits to both species is
382 expected given the close evolutionary relationships of the species. Analyses to determine
383 the best statistics to discriminate between species using reads which aligned to both
384 databases strongly indicated that difference in alignment lengths between the best
385 discriminator, shown in Figure 2a-d and Extended Data Figures 2, 3 & 4. Overall these
386 show that the difference in alignment length is a powerful indicator for both short- and
387 long-read data at any threshold ≥ ~100bp. Furthermore, and surprisingly, at this and more
388 conservative (greater difference) threshold, long-read field-sequenced reads had

389 substantially more accuracy in true- and false-positive discrimination than short-read data.
390 This suggests that this method provides a powerful means of species identification and we
391 posit that the extremely long length of 'true positive' alignments compared with the natural
392 length ceiling on false-positive alignments is largely responsible for this property.

393 **Accumulation curves for simulated identification.** 33,806 pairwise BLASTN hits
394 obtained above in identification against *A. thaliana* and *A.lyrata* genomic reference
395 databases were subsampled without replacement to simulate incremental accumulation of
396 BLASTN hit data during progress of a hypothetical sequencing experiment producing
397 10,000 reads produced in total. 1,000 replicates were used to calculate means and
398 variances for data accumulation in 0.1 log-increments from r=1 read to 10^4 reads total. For
399 each read, ΔL_I, 'number of identities bias', was calculated as the difference (number of
400 identities in *A. thaliana* alignment – number of identities in *A. lyrata* alignment). Each read
401 was assigned to *A. thaliana* or not if it ΔL_I exceeded a given threshold, repeated at four
402 possible values, $L_{threshold}$ ={0, 1, 10, 100}. Mean and aggregate (total) ΔL_I values were also
403 calculated for each replicate over the progress of the simulated data collection. Results are
404 shown in Figure 3.

405 ***De novo* genome assembly.** Short-read HTS data was assembled *de novo* using ABYSS
406 v1.9.0[35]. A hybrid assembly with both HTS and RTnS datasets was performed with
407 HybridSPAdes v3.5.0[36]. Assemblies were completed for *A. thaliana* (sample AT2a) and *A.*
408 *lyrata* (sample AL1a). Assembly statistics were calculated in Quast v4.3[37]. Completeness
409 of the final hybrid assemblies was assessed using CEGMA v2.5[38]. Results of *de novo*
410 genome assemblies are given in Extended Data Table 5. Analyses of genome contiguity
411 and correctness and conserved coding loci completeness indicated that assembly of HTS
412 data performed as expected (20x coverage produced ~25,000 contigs covering
413 approximately 82% of the reference genome at an N50 of 7,853bp). By contrast, the hybrid
414 assembly of *A. thaliana* illumina MiSeq and Oxford Nanopore MinION data significantly

415 improved on the MiSeq-only assembly: 24,999 contigs reduced to 10,644; total assembly
416 length increased to close to the length of the reference genome (119.0Mbp) with nearly
417 89% mappable; N50 and longest contig statistics both improved (N50 7,853 → 48,730bp)
418 indicating better contiguity from the addition of long reads. Completeness of coding loci as
419 estimated by CEGMA (Extended Data Table 5) greatly increased to ~99%. Long reads did
420 not compromise the accuracy of high-coverage short-read data; basewise error rates were
421 not significantly worse.

422 **Direct gene annotation of single unprocessed field-sequenced reads.** The length of
423 typical individual RTnS reads is of similar magnitude to genomic coding sequences.
424 Consequently, useful phylogenomic information could potentially be obtained by
425 annotating reads directly, without a computationally expensive genome assembly step.
426 Raw, unprocessed *A. thaliana* reads were individually annotated directly without assembly
427 via SNAP[39]. To verify which gene predictions were genuine, the DNA sequences (and 1kb
428 flanking regions, where available) were matched to available *A. thaliana* (TAIR10) genes
429 with default parameters. BLAST hits were further pruned based on quality (based on 1st-
430 quartile quality scores: alignments length bias $\Delta L_T \geq +570$bp / % identities bias ≥ +78.68 /
431 *E*-value bias ≥ 0), reducing the number of hits from 18,098 to 10,615. Sample read
432 alignments and details of SNAP output BLAST score summary statistics are given in
433 Supplementary Table 1 and encounter curves-through-time are shown in Figure 2e.

434 **Phylogenomics of raw-read-annotated *A. thaliana* genes.** Predicted *A. thaliana* gene
435 sequences were combined with a published phylogenomic dataset spanning 852
436 orthologous, single-copy genes in plants and algae[28], downsampled to 6 representative
437 taxa for speed: *Equisetum diffusum, Juniperus scopulorum, Oryza sativa, Zea mays, Vitis*
438 *vinifera* and *A. thaliana*. Our putative gene models were assigned identity based on
439 reciprocal best-hit BLASTN matching with the *A. thaliana* sequences in these alignments,
440 yielding 207 matches, of which the top 56 were used for phylogenomic analysis

441 (Supplementary Table 1), only 18 having no missing taxa in the Wickett *et al.*[28] dataset.
442 Alignments were refined using MUSCLE v3.8.31[40] and trimmed with a 50% missing-data
443 filter (using trimAL v1.4rev15[41]) then used to infer species trees in two ways: (i) single
444 gene phylogenies inferred separately (using RAxML v7.2.8[42]) under the GTRCAT
445 substitution model with 10 discrete starting trees then combined into a summary tree using
446 TreeAnnotator v.1.7.4[43]; (ii) a species tree inferred directly from the data under the
447 multispecies coalescent[44], implemented in *BEAST v2.4.4[45] (with adequate MCMC
448 performance confirmed using Tracer v1.5). A maximum clade credibility (MCC) tree was
449 produced using TreeAnnotator v.1.7.4. Phylogenies inferred by orthodox (RAxML) and
450 multispecies coalescent (*BEAST) methods are shown in Extended Data Figure 5 and
451 agreed with each other and the established phylogeny presented in Wickett *et al.*[28]
452

453 29. C., Coulouris G., Avagyan V., Ma N., Papadopoulos J., Bealer K., & Madden T.L.
454 (2008) BLAST+: architecture and applications. *BMC Bioinformatics* **10**:421.
455 30. David, M., Dursi, L.J., Yao, D., Boutros, P.B. & Simpson, J.T. (2017) Nanocall: An
456 Open Source Basecaller for Oxford Nanopore Sequencing Data. Bioinformatics
457 33(1):49-55. doi:10.1093/bioinformatics/btw569
458 31. Bolger, A. M., Lohse, M., & Usadel, B. (2014). Trimmomatic: A flexible trimmer for
459 Illumina Sequence Data. Bioinformatics 30(15):2114-2120.
460 32. Li, H. & Durbin, R. (2009) Fast and accurate short read alignment with Burrows–
461 Wheeler transform. Bioinformatics 25(14):1754–1760.
462 33. Kiełbasa SM, Wan R, Sato K, Horton P, Frith MC. (2011) Adaptive seeds tame
463 genomic sequence comparison. Genome Res. 21(3):487-93.
464 34. Sing, T., Sander, O., Beerenwinkel, N. & Lengauer, T. (2005) ROCR: Visualizing
465 classifier performance in R. Bioinformatics 21(20):3940-3941.

466 35. Simpson, J. T., Wong, K., Jackman, S.D., Schein, J.E., Jones, S.J.M. & Birol, I.
467 (2009) ABySS: a parallel assembler for short read sequence data. *Genome*
468 *research* 19(6):1117-1123.
469 36. Antipov D, Korobeynikov A, McLean JS, Pevzner PA. (2016) hybridSPAdes: an
470 algorithm for hybrid assembly of short and long reads. Bioinformatics 32(7):1009-15.
471 doi: 10.1093/bioinformatics/btv688.
472 37. Gureyvich, A., Saveliev, V., Vyahhi, N. & Tesler, G. (2013) QUAST: quality
473 assessment tool for genome assemblies. Bioinformatics 29(8):1072-1075.
474 38. Parra, G., Bradnam, K. & Korf, I. (2007) CEGMA: a pipeline to accurately annotate
475 core genes in eukaryotic genomes. Bioinformatics 23(9):1061-1067.
476 39. Korf I. (2004) Gene finding in novel Genomes. BMC Bioinformatics 5:59.
477 40. Edgar, R.C. (2004) MUSCLE: multiple sequence alignment with high accuracy and
478 high throughput. Nucleic Acids Res 32(5):1792-97.
479 41. Salvador Capella-Gutierrez; Jose M. Silla-Martinez; Toni Gabaldon. (2009) trimAl: a
480 tool for automated alignment trimming in large-scale phylogenetic analyses. Salvador
481 Capella-Gutierrez; Jose M. Silla-Martinez; Toni Gabaldon. Bioinformatics 25:1972-
482 1973.
483 42. Stamatakis, A. (2014) RAxML version 8: a tool for phylogenetic analysis and post-
484 analysis of large phylogenies. *Bioinformatics* **30**(9):1312-1313.
485 43. Drummond, A.J., Suchard, M.A., Xie, D. & Rambaut, A. (2012) Bayesian
486 phylogenetics with BEAUti and the BEAST 1.7 Molecular Biology And
487 Evolution 29:1969-1973.
488 44. Heled, J. and Drummond, A.J. (2010) Bayesian inference of species trees from
489 multilocus data. Mol. Biol. Evol. 27 (3):570-580.

45. Bouckaert, R., Heled, J., Kühnert, D., Vaughan, T., Wu, C-H., Xie, D., Suchard, MA., Rambaut, A., & Drummond, A. J. (2014). BEAST 2: A software platform for bayesian evolutionary analysis. PLoS Computational Biology, 10(4):e1003537.

Extended Data

a

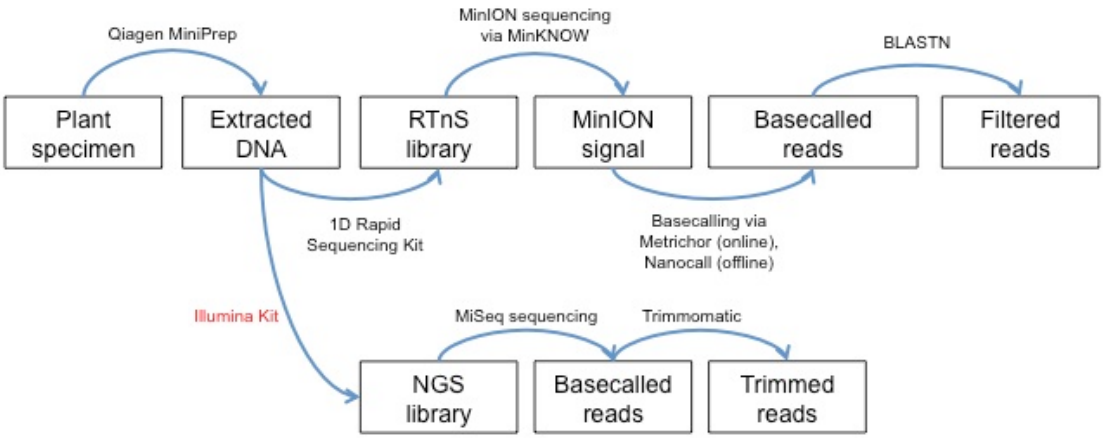

b

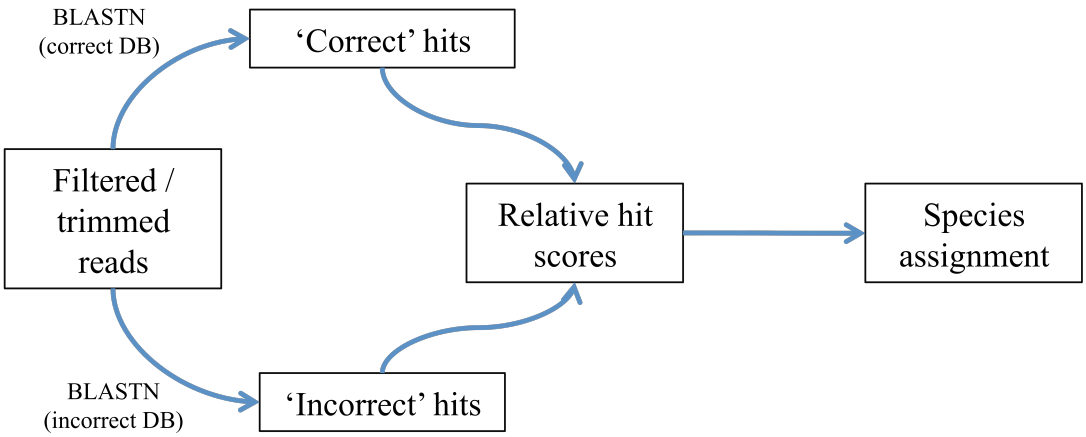

c

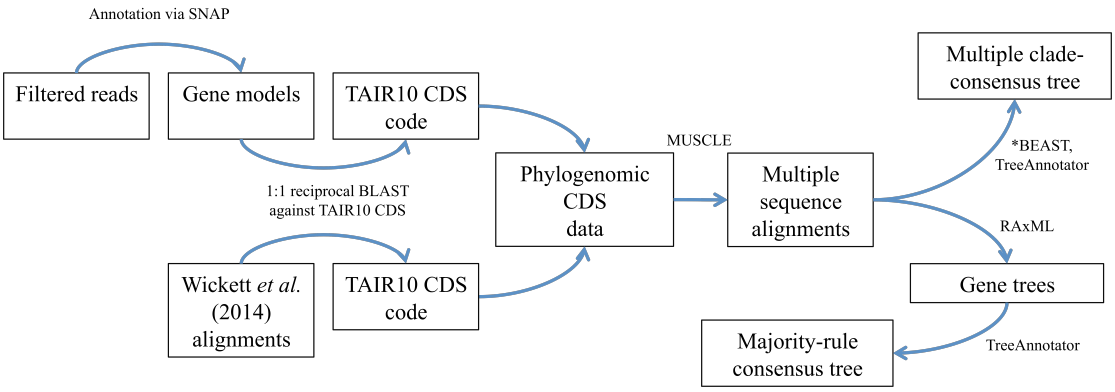

Extended Data Figure 1 | Schematic of experimental workflows. a, Sampling-to-sequencing workflow. **b,** Sample identification workflow via BLASTN. **c,** Outline for direct annotation of raw RTnS reads followed by phylogenomic inference. See Methods for details.

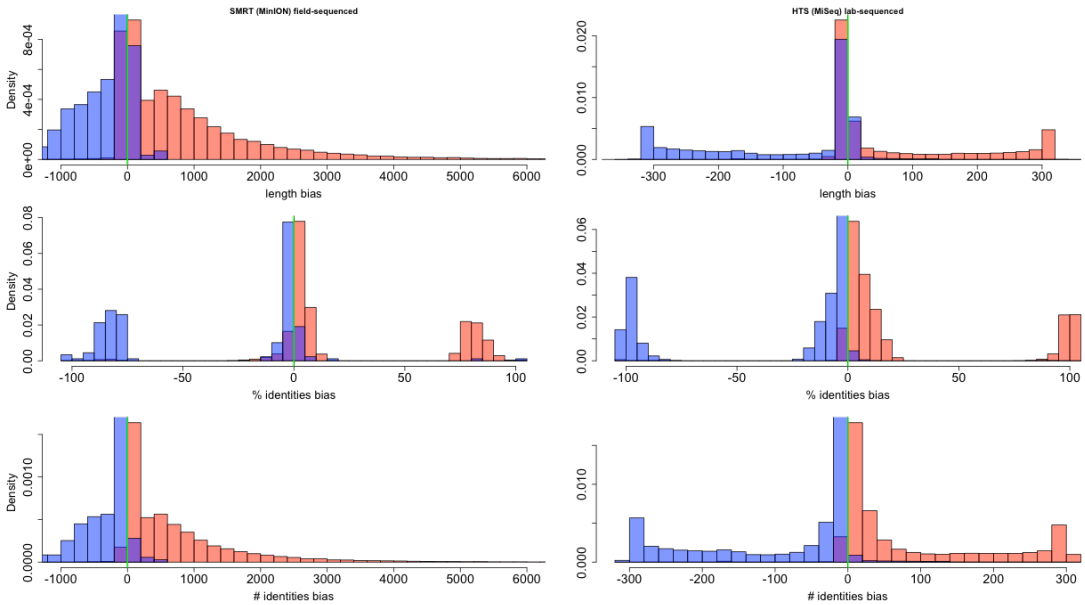

Extended Data Figure 2 | Distribution of difference statistics in BLASTN comparisons for species ID. Empirical distribution of test statistics for each-way congeneric sample ID (binary classification) using BLASTN evaluated for RTnS MinION (*left column*) and NGS MiSeq (*right column*) platforms. Difference (test) statistics were calculated for each alignment as (true positive (TP) score – false positive (FP) score) for each of: alignment length; % identities; and number of identities. Reads sequenced from *A. thaliana* samples (comprising nominal true positives and false-positives (contaminants) are shown in red; reads from *A. lyrata* samples (nominal true negatives) shown in blue. 'True' and 'false' distributions' overlap is small, while alignment length and number of identities' distributions are both unimodal, showing a simple cutoff-based classifier should perform well to discriminate between 'true' and 'false' cases.

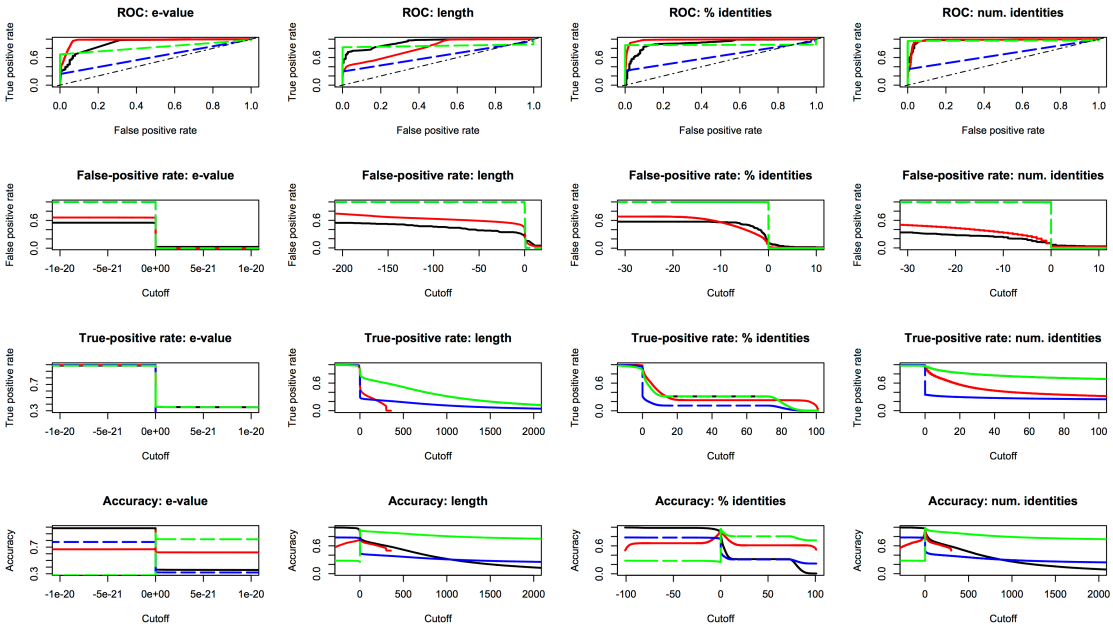

Extended Data Figure 3 | Performance of difference statistics in BLASTN comparisons for species ID. Performance of test statistics for each-way congeneric sample ID (binary classification) using BLASTN evaluated for MinION (*black*) and MiSeq (*red*) platforms. Difference (test) statistics were calculated amongst reads matching both databases for each alignment as (true positive (TP) score – false positive (FP) score) for each of e-value, length, % identities and number of identities. Reads matching only one or neither database were additionally included with either 'all-false' encoding (dashed green line) or mixed false and true encoding depending on sample origin (blue line; see Methods and Supplementary Information for details). RTnS reads' true- and false-positive rates are comparable to, and in some cases better than, NGS reads' performance; while the longer length of RTnS reads permits the use of high thresholds where greater confidence is desired (perhaps in the case of very closely related specimens). *Top row:* true-positive (TP) vs false-positive (FP) rate; classical receiver operating curve. *Second row:* FP rate with varying test statistic threshold. *Third row:* TP rate with varying test statistic threshold. *Bottom row:* Accuracy with varying test statistic threshold. Accuracy estimated as (TP+TN / (P + N)). *Columns (L-R):* Difference statistics for *e*-value, total alignment length, % identities, and number of identities, respectively.

534

535

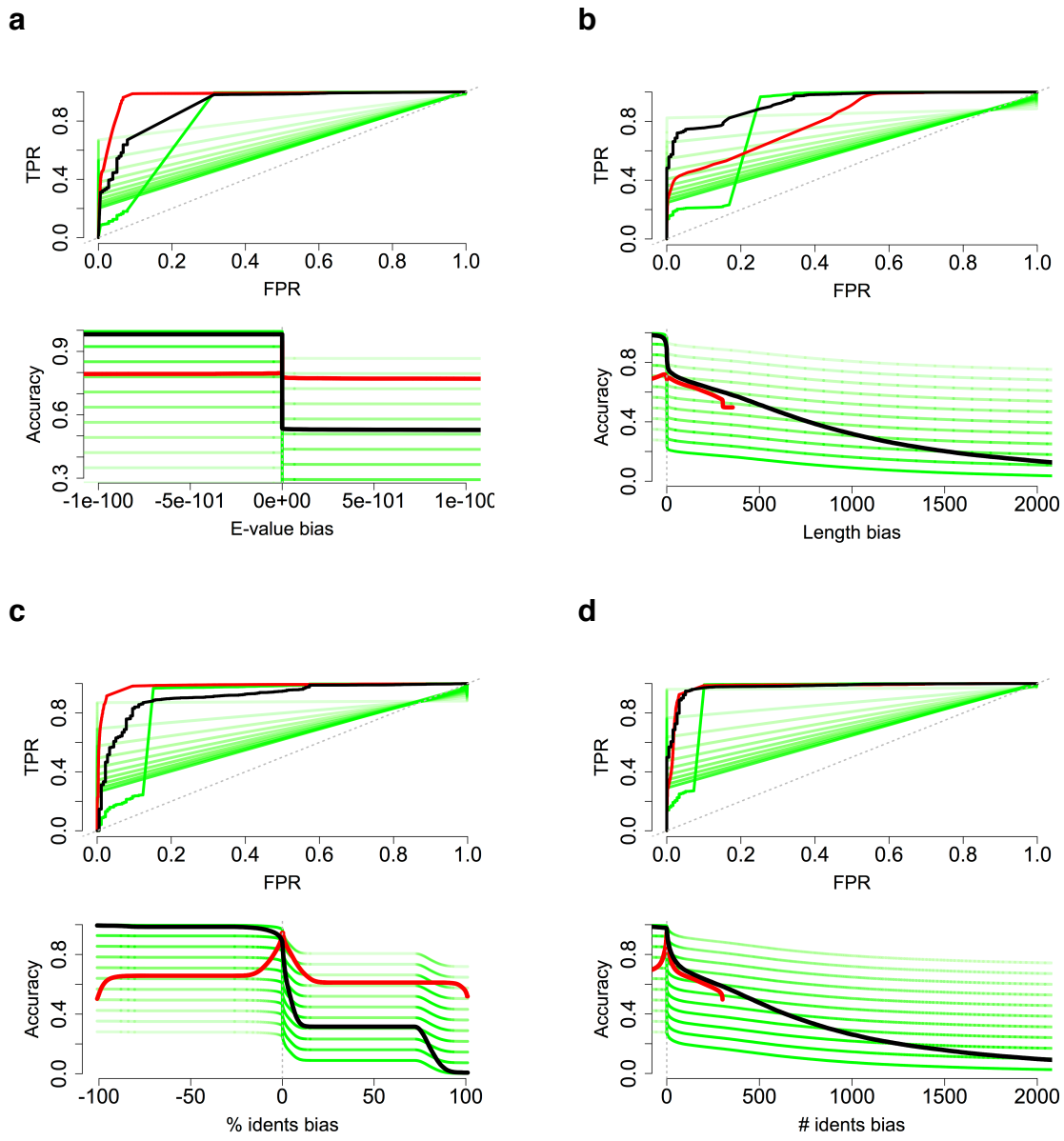

536

537 **Extended Data Figure 4 | Modelling potential effect of incorrectly estimated TN/FN**
538 **proportions.** Red and black lines show empirically estimated statistical performance for species
539 ID via BLASTN comparison of HTS and RTnS reads respectively (as for Extended Data Figure 3;
540 see Methods for details). Reads that produced no hits to either database might represent false
541 negatives (sequencing error, or genomic regions not represented in the reference genome BLAST
542 databases) or true negatives (sequencing contaminants and sequencer noise). These
543 nonmatching reads were to reflect 'true negative':'false negative' ('TN:FN') mixtures in 10%

544 increments shown from light to dark green shading. Plots (**a-d**) show results for bias statistics in *E*-
545 value; total alignment length; % identities; and total alignment identities, respectively. Extreme
546 TN:FN mixtures still display adequate true-positive vs. false-positive rates; empirical data is
547 approximated by the 30% TN:FN mixture, approximately reflecting the proportions of *A. lyrata* to *A.*
548 *thaliana* nonmatching reads in the dataset.
549

549

550 **a**

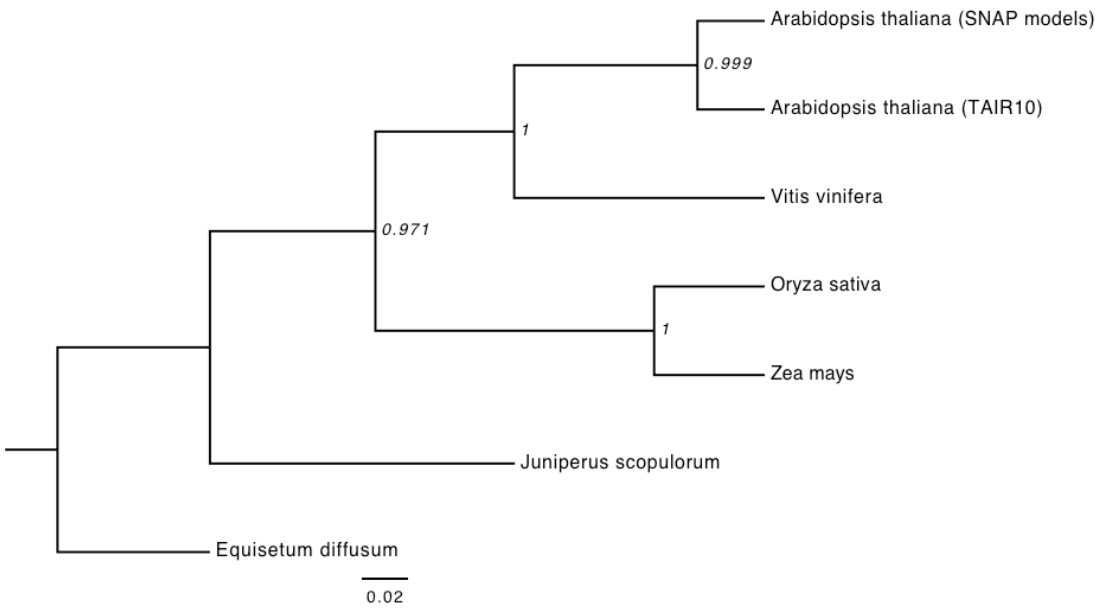

551

552 **b**

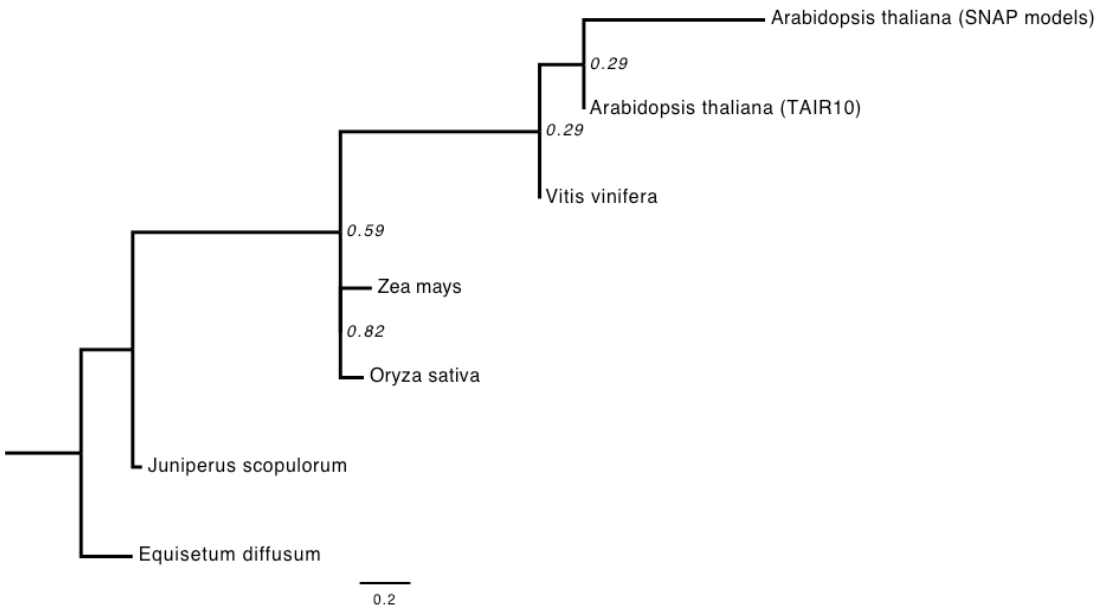

553

554

555 **Extended Data Figure 5 | Phylogeny of species spanning major plant groups.** Putative coding
556 sequences recovered from single, unassembled raw RTnS reads using SNAP *ab initio* gene
557 prediction could be aligned to existing phylogenomic data from other taxa and used to infer a
558 phylogeny consistent with accepted plant relationships. **a,** Multispecies coalescent species tree
559 inferred from 18 gene trees (genes predicted directly from raw nanopore reads). Inferred using

560 multispecies coalescent implemented in BEAST 2.4.4; **b,** consensus species tree inferred by
561 majority-rule from 18 gene trees, inferred with RAxML 7.2.8.
562

562

563

564

565 **Extended Data Table 1 | List of field-sequencing equipment.**

Item / model	Quantity	Supplier
Laptops, Portege R830-1DZ	2	Toshiba
Laptop, MacBook Pro	1	Apple
Portable firewire HDD, 1Tb	2	LaCie
Portable AC generator, IMPAX IM800I 700W	1	ScrewFix
Thermal control textiles (socks) for MinION	Pair	ScrewFix
AC extension plugs, 4-way, 3-20M	3	Argos
Portable folding tables	2	Argos
Weather meter, Kestrel 5500	1	KestrelMeters
Fluorometer, Quantus	1	Promega
Water bath, GD100	1	Grant
Microcentrifuge, 5415C	1	Eppendorf
Glass thermometers, 300mm, range 263.3-383.3ºK	2	
Arduino Uno	1	Maplins
Themal transducers, LM335AZ	4	RS Components
Polystyrene thermal control boxes, various sizes	3	
Freezer coolpacks	14	
Pipettes, Gilson:	-	
P2	1	ThermoFischer
P20	1	ThermoFischer
P200	1	ThermoFischer
P1000	1	ThermoFischer
Waste containers	2	
Laboratory consumables:	-	
PCR tubes, thin-walled	Box	ThermoFischer
Eppendorf tubes, 1.5ml DNA lo-bind	Box	ThermoFischer
Eppendorf tubes, 2.0ml DNA lo-bind	Box	ThermoFischer
Plastic pestles	20	
Sterilized sand	5g	
Reagent tubes, screw-top, 50ml	10	ThermoFischer

566

567

567

568

569 **Extended Data Table 2 | Performance of MinION sequencing runs**

Species		***A. thaliana***	***A. thaliana***	***A. lyrata***	***A. lyrata***
Reaction chemistry		R7.3, 1D	R9, 1D	R7.3, 1D	R9, 1D
Run IDs		2507 2126 3637	5913 2144 0509	4901 1842 1201	1222 5458 1958 0824 2912 5201
Start time		18/05/2016 21:36	18/05/2016 18:21	19/05/2016 16:10	19/05/2016 16:39:20
Latest read*		19/05/2016 15:17:00	19/05/2016 15:18:39	24/05/2016 01:14	22/05/2016 07:08:56
Disc space (raw)		2.9Gb	106.8Gb	3.0Gb	35.1Gb
Metrichor ID		115360	115459	115375	115432
# reads		4,152	92,693	2,387	23,452
Yield (bp):					
	total	7,351,585	233,244,147	16,092,487	46,118,754
	mean	1,771	2,516	6,742	1,967
	median	586	1,396	120	305
	maximum	434,377	170,598	1,114,970	177,310
	N25	19,244	9,651	574,112	24,254
	N50	4,771	4,410	309,034	7,926
	N75	2,041	2,121	62,360	3,374

570

571 Data produced with field-extracted and field-sequenced in conditions ranging from 6-14ºC and up
572 to 100% humidity, producing genome-scale sequence data despite several pauses in sequencing
573 to dismantle, relocate, and reassemble equipment. The two latest sequencing runs (*A. lyrata*
574 samples) performed markedly worse than the two earliest runs (*A. thaliana)*, possibly due to the
575 impact of storage temperature (passively controlled, and steadily rising over the week) on reagent
576 performance. Yield summary statistics refer to untrimmed raw reads, including phage-lambda
577 experimental control in the case of *A. thaliana* R9 data (filtered from subsequent steps). See
578 Methods for details. Note: *Final *A. lyrata* sequencing phase performed in laboratory owing to time
579 constraints on-site.

580

580

581

582

583 **Extended Data Table 3 | Statistics of reference genomes used**

Species	*Arabidopsis lyrata ssp. petraea*	*A. lyrata*	*A. thaliana*
Version	1.0	1.0	TAIR10
Date accessed	25/05/2016	17/05/2016	17/05/2016
Accession / ID	NCBI: assembly=GCA_000524985.1	NCBI: genome=493 genome_assembly=29434	NCBI: genome=4 genome_assembly=22492
Total assembly length	202,972,003	206,667,935	119,667,750
Total gap length	20,456,163	22,960,134	185,644
Number of scaffolds	281,536	695	7
Scaffold N50	7,848	24,464,547	23,459,830
Scaffold L50	6,426	4	3
Number of contigs	369,168	3,645	102
Contig N50	2,321	227,391	11,194,537
Contig L50	16,831	247	5
Total chromosomes & plasmids	0	0	7

584

585 *A. thaliana* TAIR10 release is considerably more complete than either of the draft *A. lyrata*

586 assemblies.

587

587

588

589

590 **Extended Data Table 4 | Sample identification via BLASTN**

Sample	*A. thaliana*	*A.lyrata*	*A. thaliana*	*A.lyrata*
"TRUE" database	*A. thaliana*	*A.lyrata* combined*	*A. thaliana*	*A.lyrata* combined*
"FALSE" database	*A.lyrata* combined*	*A. thaliana*	*A.lyrata* combined*	*A. thaliana*
Source data	ONT 1D	ONT 1D	MiSeq	MiSeq
# Reads, total	91,715	25,839	9,476,598	9,659,489
# Reads with BLASTN hits:				
1-way TRUE†	10,322	76	2,140,403	2,907,921
1-way FALSE‡	378	2	53,056	24,329
2-way BOTH§	22,386	101	7,098,032	6,256,969
0-way ZERO¶	58,629	25,660	185,107	470,270
Proportion of reads:				
1-way TRUE	*0.113*	*0.003*	*0.226*	*0.301*
1-way FALSE	*0.004*	*0.000*	*0.006*	*0.003*
2-way BOTH	*0.244*	*0.004*	*0.749*	*0.648*
0-way ZERO	*0.639*	*0.993*	*0.020*	*0.049*
Biases #:				
Mean length	1,323.87	698.25	83.61	108.99
Mean identities	1,115	575	96	117
Mean % identities	37.97	61.41	30.16	42.38
Mean E-*values*	4.80E-07	1.05E-04	1.07E-08	3.52E-09

591

592 Individual RTnS and NGS reads were aligned to *A. thaliana* and *A. lyrata* databases (designated
593 TRUE or FALSE depending on sample origin) with BLASTN, keeping the single best-hit alignment
594 for each database. More '1-way' (only one database matched) hits to TRUE than FALSE
595 databases accumulated in all sample / technology combinations. Amongst '2-way' hits, positive
596 differences in the metrics were consistent with correct sample identification. For RTnS reads
597 differences between TRUE and FALSE hits were considerably larger than amongst HTS reads (by
598 an order of magnitude for length or number of identities), showing that confident identification could
599 be made with fewer RTnS reads. Notes: **A. lyrata* and *A. lyrata ssp. petraea* databases combined,
600 see Methods; †Total number of reads matching only conspecific database ('true-positives'); ‡Total
601 number of reads matching only pairwise-compared database ('false-positives' in the case of a
602 mixed /multiplexed sample, or 'false-negatives' in the case of a single sample); §Total number of

603 reads matching both databases; ¶Total number of reads with no hits in either comparison, e.g.
604 'false-negatives'; #Difference statistics for each query read calculated as (score conspecific
605 comparison – score congener comparison), for BLASTN alignment length, alignment identities,
606 alignment % identities and *E*-value; ✩Mean bias across all reads.
607

607

608

609

610 **Extended Data Table 5 | Performance of *de novo* genome assembly**

Species	***Arabidopsis thaliana***		***A. lyrata ssp. petraea***	
Data	**MiSeq**	**MiSeq + MinION**	**MiSeq**	**MiSeq + MinION**
Assembler *	**Abyss**	**hybridSPAdes**	**Abyss**	**hybridSPAdes**
Illumina MiSeq NGS reads, 300bp paired-end	8,033,488	8,033,488	8,143,010	8,143,010
NGS total yield	2,418,079,888	2,418,079,888	2,451,046,010	2,451,046,010
Oxford Nanopore MinION RTnS reads, R7.3 + R9, N50 ~ 4,410bp	n/a	96,845	n/a	25,839
RTnS reads total yield	n/a	240,597,532	n/a	62,211,241
# contigs	24,999	10,644	37,568	85,599
Largest contig	89,717	413,462	101,114	38,313
Total length	106,455,313	119,031,857	151,562,895	117,256,694
Reference length	*119,667,750* †	*119,667,750*	*183,707,801*‡	*183,707,801*
GC content (%)	35.97	36.20	36.16	36.55
N50 §	7,853	48,730	9,605	1,686
Unaligned length	7,121,882	6,737,059	36,669,847	35,287,390
Genome fraction (%)	82.0	88.7	53.4	43.7
Duplication ratio	1.01	1.058	1.17	1.02
# N's per 100 kbp	1.72	5.41	0.22	7.09
# mismatches / 100 kbp	518	588	1,297	1,097
# indels / 100 kbp	120	130	334	271
Largest alignment	76,935	264,039	44,515	17,201
Total aligned length	98,382,255	108,086,256	100,502,092	80,814,492
Coding loci completeness¶*:*				
# genes, 'complete'	**219**	**245**	n/a	n/a
% genes, 'complete'	88.31%	98.79%		
# genes 'partial'	**238**	**246**	n/a	n/a
% genes, 'partial'	95.97%	99.19%		

611

612 Field-extracted DNA material was of sufficient quality to enable a *de novo* assembly with lab-
613 sequenced NGS data. Furthermore, field-sequenced RTnS reads considerably augmented the
614 NGS data in hybrid assembly, greatly improving contiguity and estimated coding loci coverage
615 substantially without substantially raising basewise error rates. Notes: **de novo* genome

616 assemblies used either lab-sequenced short-read HTS data only (Abyss) or both HTS and field-
617 sequenced RTnS datasets (Hybrid-SPAdes). †TAIR10 release. ‡INSDC: *A. lyrata*:
618 ADBK00000000.1 (Hu *et al.,* 2011); *A. lyrata ssp. petraea*: BASP00000000.1 (Akama *et al.*, 2014).
619 §Assembly statistics calculated using QUAST 4.0. ¶Approximate completeness of coding loci
620 assessed via CEGMA. See Methods for details.
621